JOURNAL OF MOLECULAR SPECTROSCOPY **148,** 226–242 (1991)

Analysis of BaI $C^2\Pi$–$X^2\Sigma^+$ (0, 0) Band for High Rotational Levels

D. ZHAO, P. H. VACCARO,[1] A. A. TSEKOURAS, C. A. LEACH, AND R. N. ZARE

Department of Chemistry, Stanford University, Stanford, California 94305

Using laser-induced fluorescence, rotationally resolved spectra of the BaI $C^2\Pi$–$X^2\Sigma^+$ (0, 0) band have been observed for J'' values from 339.5 to 486.5 in the P_{12}, 57.5 to 494.5 in the P_2, and 124.5 to 370.5 in the R_{21} branches. The BaI molecules are formed from the reaction of Ba and HI. These new data have been combined with lower J'' lines ($J'' < 156.5$) previously measured by Johnson, Noda, McKillop, and Zare [*Can. J. Phys.* **62,** 1467–1477 (1984)]. All the high J'' lines have been unambiguously assigned, although lines in the P_{12} branch between J'' values of 156.5 and 338.5 have not been observed. A rotational analysis has been carried out by performing a nonlinear least-squares fit to the eigenvalue differences of the model Hamiltonians for the upper and lower states. In addition, a further least-squares fit was carried out including all the (0, 0) band data and the six $X^2\Sigma^+$ $v = 0$ microwave rotational transitions of Törring and Döbl [*Chem. Phys. Lett.* **115,** 328–332 (1985)]. Six out of the twelve rotational branches form blue-shaded bandheads at J'' well over 400. These bandheads are caused by the difference between the centrifugal distortion constants D' and D''. The model Hamiltonians are able to describe the transitions, although the highest rotational energy (about 6300 cm^{-1}) is much larger than the energy separation of the vibrational levels (about 150 cm^{-1}).

1. INTRODUCTION

The spectroscopy of BaI is an excellent example of some of the new achievements made possible by advances in laser technology. Before the age of laser spectroscopy, there was no information about the rotational structure of the spectrum of this heavy molecule, although vibrational information was available. BaI vibrational bands were first observed by Walters and Barratt (*1*), and later a more comprehensive study was carried out by Patel and Shah (*2*). In this paper we show that the bandhead positions are tens of wavenumbers away from the band origins, thus making accurate determinations of the band origins difficult without rotational analysis. In 1981, Johnson *et al.* assigned the BaI $C^2\Pi$–$X^2\Sigma^+$ (0, 0) band using population-labeling optical–optical double resonance (PLOODR) (*3*) (see also (*4*)). Later, selectively detected laser-induced fluorescence (SDLIF) was used to measure more than 400 lines involving J'' up to 155.5 (*5*). In these studies (*3–5*), a collimated beam of BaI from an oven source (~1300 K) was used. No bandheads were observed. By collimating the BaI beam, the Doppler width was reduced to below 150 MHz. Rotational constants B' and B'' were found to be essentially equal to each other. These studies were done to facilitate the investigation of the dynamics of the reaction Ba + HI → BaI + H, where the measurement of the opacity function of the reaction is made possible by the mass combination (kinematic constraint) (*6*). To extend these studies, we have constructed

[1] Present address: Department of Chemistry, Yale University, New Haven, CT 06511.

0022-2852/91 $3.00

a crossed-beam apparatus (*7*). Under these conditions the reaction of Ba and HI yields highly rotationally excited BaI products, whose J'' values are much larger than those observed in a thermal BaI beam. Therefore, an additional spectroscopic study was needed before the rotational energy distribution of the product BaI could be determined. In this paper, we report the assignment of rotational transitions with J'' up to 494.5. We also present an improved set of molecular constants for the BaI $C^2\Pi$–$X^2\Sigma^+$ (0, 0) band. In general, a J value of 50 or 100 is referred to as high J, but here we have observed and assigned rotational spectra for J'' up to nearly 500!

The BaI $C^2\Pi$–$X^2\Sigma^+$ transition involves the transfer of an electron between two nonbonding orbitals primarily centered on the Ba atom (*8*). Hence the shape and internuclear distances for the two potential energy curves are similar. This results in Franck–Condon factors that strongly favor $\Delta v = 0$ transitions. The (v, v) vibronic bands are separated by only 6 cm^{-1} as expected from the difference in vibrational constants of the $C^2\Pi$ and $X^2\Sigma^+$ states. The two spin–orbit subbands are separated by 756 cm^{-1} and do not overlap. The rotational constants (B' and B'') are very small, approximately 0.027 cm^{-1}, because of the large mass of both barium and iodine atoms. In addition, the spin–rotation splitting of the lower state and the Λ-doubling of the upper state cause each spin–orbit subband to have six rotational branches. With J'' levels up to 494.5 populated, the rotational spectrum of each $\Delta v = 0$ vibronic band spans about 75 cm^{-1}. As a result, the rovibrational spectrum of BaI $C^2\Pi$–$X^2\Sigma^+$ is very congested, with as many as 300 lines per wavenumber.

As mentioned before, Johnson *et al.* (*3–5*) assigned the $C^2\Pi$–$X^2\Sigma^+$ (0, 0) band for J'' up to about 155.5. We have observed about 150 lines with J'' between 339.5 and 494.5 for each of the P_2 and P_{12} branches using undispersed laser-induced fluorescence (LIF) detection of BaI molecules formed from a crossed-beam reaction of Ba and HI. In addition we used SDLIF to measure the P_2 branch with J'' between 57.5 and 313.5 and the R_{21} branch between 124.5 and 370.5. These new lines could not be assigned by extrapolation based on the molecular constants of Johnson *et al.* However, the J'' numbers of these lines could be determined from a nonlinear least-squares fit to model Hamiltonians for the upper and lower states that involved all observed transitions.

2. EXPERIMENTAL DETAILS

a. Undispersed Laser-Induced Fluorescence (LIF)

The experimental apparatus was similar to that used for studying the dynamics of Ba + HI (*7*). Figure 1 shows a schematic diagram of the reaction chamber. A detailed description of the crossed-beam scattering apparatus has been given elsewhere (*7*).

In brief, a mixture of HI and carrier gas was expanded through a 100 μm-diameter nozzle to form a supersonic HI ($X^1\Sigma^+$) beam. At the interaction region the beam diameter was about 8 mm, with a beam flux of about 10^{17} particles cm^{-2} sec^{-1}. A nearly effusive Ba ($^1S_0$) beam was produced by a high temperature oven source and collimated by several apertures before entering the scattering chamber. The beam diameter was about 8 mm at the intersection with the HI beam. The Ba beam had a flux of the order of 10^{16}–10^{17} particles cm^{-2} sec^{-1}.

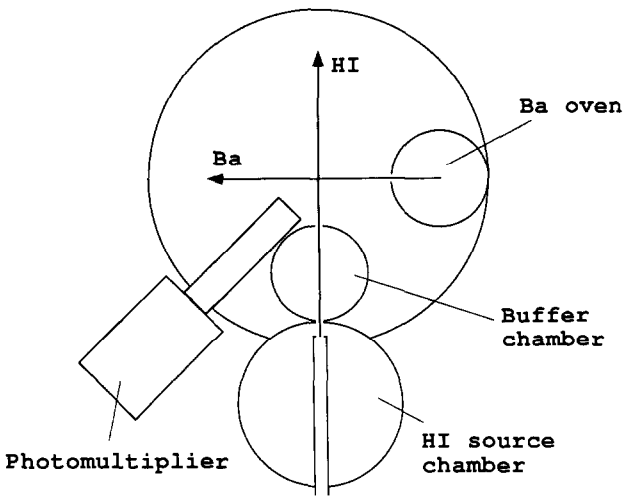

FIG. 1. Schematic cross section through the reaction chamber. The laser beam crosses the HI and Ba reaction region perpendicular to the plane of the diagram.

The excitation laser was a single-mode CW ring dye laser (Coherent 699-29) that contained Rhodamine 560 dye (Exciton) and was pumped by a mainframe argon ion laser (Spectra-Physics 171-17, 6W at 514.5 nm). The actively stabilized laser linewidth was specified to be less than 1 MHz. The laser beam was actively power stabilized, expanded to about 5–7 mm diameter and attenuated to about 3–5 mW before entering the reaction chamber. The laser beam crossed the interaction region perpendicular to the plane defined by the HI and Ba beams. An iodine spectrum was recorded for absolute wavenumber calibration (*9*).

The fluorescence signal was collected at $f/1.5$ by a set of optics placed in the plane of the two scattering beams and perpendicular to the laser excitation beam. After being imaged onto a slit of 8×12 mm, the signal was recollimated and filtered by a narrow band-pass interference filter (Oriel). The fluorescence was detected by a cooled photomultiplier (Centronic Q4283 RA at $-20°C$), and the signal was fed into a lock-in amplifier (PAR 124A with 116 preamplifier) referenced at the frequency (667 Hz) at which the laser beam was mechanically chopped.

b. Selectively Detected Laser-Induced Fluorescence (SDLIF)

To obtain a unique assignment for the P_2 branch, a beam–gas experiment was carried out to measure some lines at J'' values in between those recorded by Johnson *et al.* and those observed in the crossed-beam experiment. This was possible because the beam–gas experiment provided a lower and wider range of collision energies and greater signal when compared to the crossed-beam reaction. The increased signal allowed the use of SDLIF to isolate members of rotational branches which could not be measured by undispersed LIF because of overlap with other rovibronic transitions.

The experimental setup used was the same as already described for the beam–beam

reaction with the following differences. Room temperature HI gas was admitted into the reaction chamber and maintained at a pressure of about 1.5×10^{-3} Torr. This pressure, while possibly compromising the nascent nature of the BaI population distributions, presented no difficulties for the spectroscopic measurements. A laser power of between 25 and 250 mW was used. A 1-m monochromator (Interaction Technology CT103) was used so that only the fluorescence signal from the Q_{21} and R_2 branches was detected (*5*) (also see (*10*)). The signal was collected at about $f/7$. Both the entrance and exit slit widths were set to between 150 and 300 μm so that the full width at half-maximum of the detection window was in the range of 3–6 cm^{-1}.

Similarly, the R_{21}-branch line positions were measured by selectively detecting fluorescence from transitions in the P_{21} and Q_2 branches.

3. RESULTS

Using the crossed-beam reaction of Ba with HI, we measured the rotationally resolved $C^2\Pi$–$X^2\Sigma^+$ (0, 0) spectrum of the product BaI formed in $X^2\Sigma^+$ ($v'' = 0$). Figure 2 shows a spectrum of some P_{12}-branch members, measured with N_2 as a carrier gas in the supersonic HI beam. In this spectrum the linewidths are dominated by hyperfine structure, which is not resolved because of the Doppler effect associated with the BaI molecules. Figure 3 shows a Fortrat diagram of the complete $C^2\Pi_{1/2}$–$X^2\Sigma^+$ (0, 0) subband. The position of the previous spectrum can now be located on the diagram. The transitions occur just below the bandhead in the P_{12} branch.

The Fortrat diagram of the subband $C^2\Pi_{3/2}$–$X^2\Sigma^+$ (0, 0) is almost identical to that of the $C^2\Pi_{1/2}$–$X^2\Sigma^+$ (0, 0) subband shown in Fig. 3 except that it is shifted by 756 cm^{-1}. We have observed all six bandheads in our experiments. The experimental wavenumbers are given in Table I.

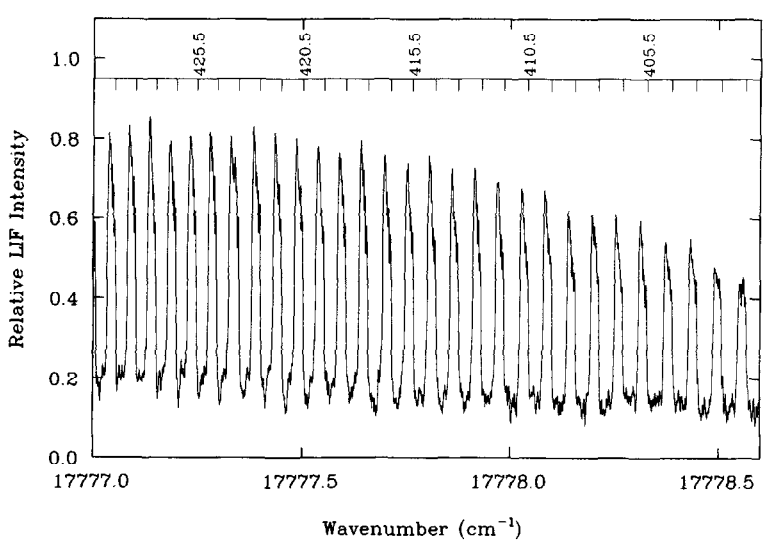

FIG. 2. Example high J'' spectrum from the P_{12} branch of the BaI $C^2\Pi$–$X^2\Sigma^+$ (0, 0) band for J'' values between 429.5 and 401.5.

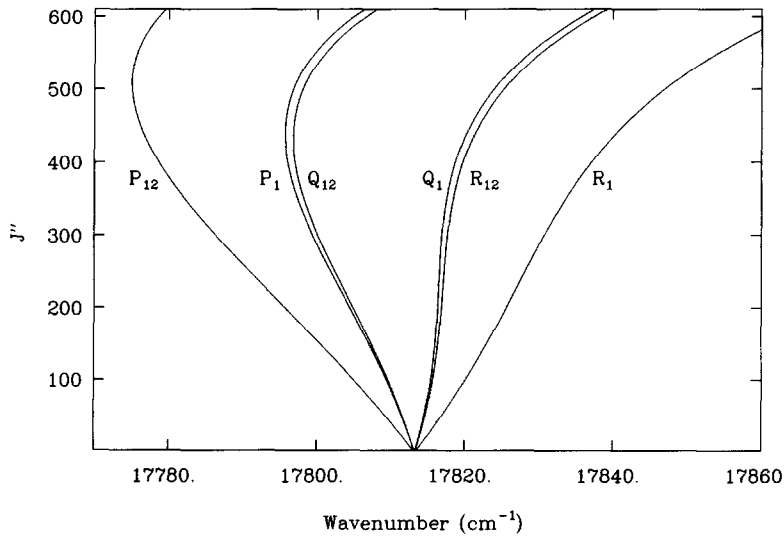

FIG. 3. Fortrat diagram of the BaI $C^2\Pi_{1/2}$–$X^2\Sigma^+$ (0, 0) subband.

The collision energy of the reaction was changed by varying the composition of the carrier gas in the supersonic expansion of the HI beam. The limited range of collision energies available during a particular experiment yielded a very narrow rotational population distribution ($\sim$50 J'') for the $v = 0$ BaI product. This allowed the measurement of lines in P_2 with J'' from 347.5 to 494.5 and in P_{12} with J'' from 339.5 to 486.5. Higher J'' lines could not be measured because they are too close to the bandhead and lower J'' lines could not be observed because they overlap with those in the (1, 1) band. The explanation of why the P_{12} branch was only measured to lower J'' values than the P_2 branch is that the former has a larger hyperfine splitting (*11*).

TABLE I

Experimental and Calculated Bandhead Positions and Corresponding J'' Values for the BaI $C^2\Pi$–$X^2\Sigma^+$ (0, 0) Band

Branch	Experimental Wavenumber (cm^{-1})	J''[a]	Calculated Wavenumber[a] (cm^{-1})	J''[b]	Calculated Wavenumber[b] (cm^{-1})
P_{12}	17775.076	507.5	17775.056	508.5	17775.050
P_1	17795.127	438.5	17795.665	442.5	17795.428
Q_{12}	17796.213	432.5	17796.756	436.5	17796.538
P_2	18529.547	508.5	18529.540	508.5	18529.541
P_{21}	18552.498	441.5	18552.603	444.5	18552.389
Q_2	18553.569	435.5	18553.701	438.5	18553.503

[a] Calculated using the molecular constants from Table II.

[b] Calculated using the molecular constants from Table III.

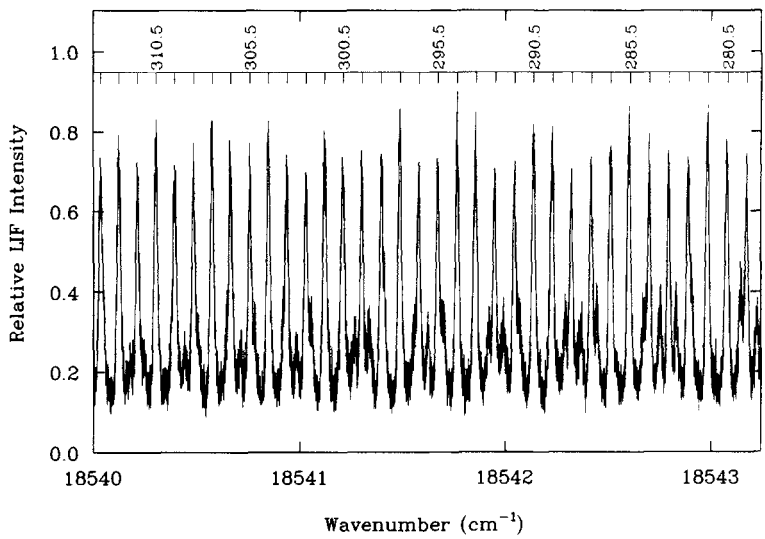

FIG. 4. Example SDLIF spectrum of the P_2 branch of the BaI $C^2\Pi$–$X^2\Sigma^+$ (0, 0) band for J'' values between 313.5 and 278.5.

An SDLIF experiment was carried out to confirm the assignment of the P_2 branch. Figure 4 shows a typical SDLIF spectrum from the P_2 branch of the (0, 0) band. In this spectrum the linewidths arise from unresolved hyperfine structure, broadened by the Doppler effect associated with the BaI products formed under beam–gas conditions. In addition, laser saturation and in some cases overlap with other rovibronic transitions contribute to the observed widths. Similarly, we observed the R_{21} branch from J'' equal to 124.5 to 370.5.

Johnson *et al.* did not see any perturbation in their analysis of BaI $C^2\Pi$–$X^2\Sigma^+$ (0, 0) for J'' below 156.5. We extend their conclusion for all the transitions we have observed up to J'' of 494.5.

All new line positions are collected in the Appendix.

4. ANALYSIS

The model Hamiltonians for the upper and lower states have been described in detail elsewhere (*12*). Briefly, the upper $C^2\Pi$ state is characterized by a large spin–orbit splitting ($\sim$756 cm^{-1}), which greatly exceeds the rotational constant B' ($\sim$0.027 cm^{-1}). Consequently, this state is well described by Hund's case (a) coupling. In addition, interaction with $^2\Sigma$ states lying above and below the $C^2\Pi$ state causes Λ-doubling of each level, characterized by the Λ-doubling parameters, o', p', and q'. In this treatment the value of o' is fixed using the unique perturber approximation while the values of p' and q' are allowed to vary (*12*). Centrifugal distortion is included by introducing the additional parameters, A'_D, q'_D, p'_D, D', and H'. The $X^2\Sigma^+$ state belongs to Hund's case (b) coupling and its rotational lines are split by spin–rotation coupling, characterized by the parameter γ''. In addition to the band origin ν_0, the rotational constant of the ground state B'' and γ'', we also included the parameters D'' and H'' to account for centrifugal distortion. The higher-order parameters are necessary to describe the J'' dependence. Using the constants of Johnson *et al.* for the (0, 0) band

TABLE II

Molecular Constants (in cm^{-1}) for the BaI $C^2\Pi$–$X^2\Sigma^+$ (0, 0) Band Determined from a Least-Squares Fit Including Only the Optical Data

ν_0	1.81782460(305) x 10^4 [a]
A'	7.822443(611) x 10^2
A_D'	-5.175(408) x 10^{-5}
B'	2.675208(679) x 10^{-2}
D'	3.5587(670) x 10^{-9}
H'	7.023(712) x 10^{-16}
q'	-6.933(1020) x 10^{-5}
q_D'	1.9166(601) x 10^{-10}
p'	7.1494(176) x 10^{-3}
p_D'	-1.317(111) x 10^{-8}
o'	2.6131 x 10^1 calculated
o_D'	-4.814 x 10^{-5} calculated
B"	2.677067(406) x 10^{-2}
D"	3.7253(651) x 10^{-9}
H"	6.734(698) x 10^{-16}
γ"	2.499(21) x 10^{-3}

[a] Two standard deviation uncertainties derived from the fit are given in parentheses in units of the last significant figure.

as a starting point, all the experimentally measured lines were fit to the eigenvalue differences between the upper and lower state Hamiltonians at certain J' and J'' values according to the selection rules of each branch.

When only the high J'' lines in the P_2 and P_{12} branches had been recorded, we had hoped to assign these using the information already available from the spectroscopic study of Johnson *et al.* In the P_{12} branch we had J'' from 8.5 to 155.5 and 150 lines from 339.5 to 486.5. We found that these lines could be assigned without additional information.

In the P_2 branch we had 150 lines at high J'' but this time only 10 scattered lines at low J'' (6.5–49.5). We found that two assignments were possible. The correct assignment was determined by an additional SDLIF experiment in which lines with intermediate values of J'' were recorded. Members of the R_{21} branch were also measured by SDLIF and assigned to J'' values between 124.5 and 370.5.

We carried out a nonlinear least-squares fit to the model Hamiltonians using 14 adjustable parameters. The molecular constants determined from this least-squares fit are shown in Table II. The number of figures quoted is required to reproduce the calculated residuals given in the Appendix (*13*). The residuals are also given in Fig. 5. Their standard deviation is 0.00236 cm^{-1}. If we change the assignment of the high J'' lines in the P_{12} branch by one quantum, the standard deviation of the fit becomes 0.0045 cm^{-1} and an obvious systematic error appears in the residuals for the incorrectly assigned branch. Figure 6 shows the residuals for a least-squares fit carried out with

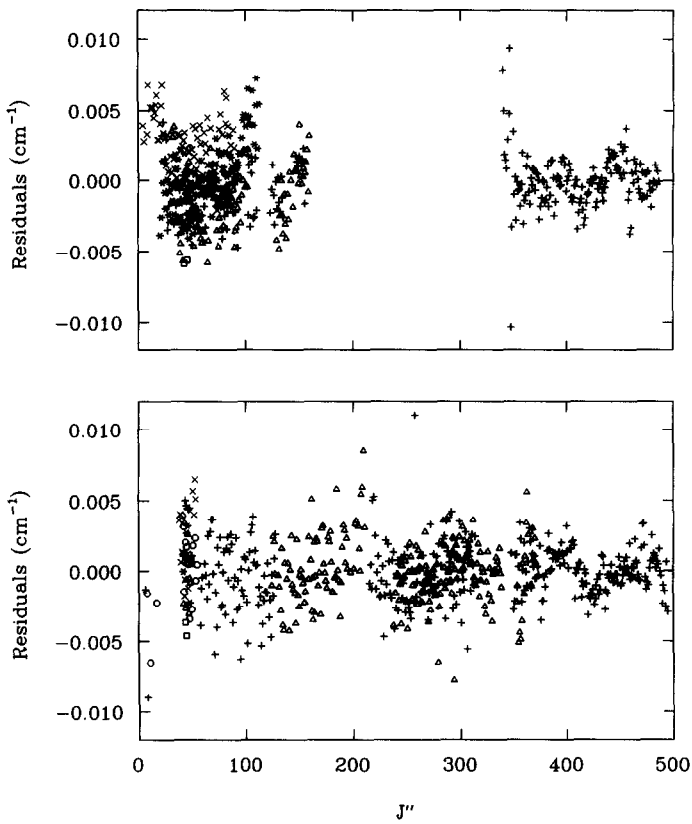

FIG. 5. Residuals of the least-squares fit for the $C^2\Pi_{1/2}$–$X^2\Sigma^+$ subband (upper panel: P_1 (○), P_{12} (+), Q_1 (∗), Q_{12} (×), R_1 (△), and R_{12} (□)) and the $C^3\Pi_{3/2}$–$X^2\Sigma^+$ subband (lower panel: P_{21} (○), P_2 (+), Q_{21} (∗), Q_2 (×), R_{21} (△), and R_2 (□)).

the P_{12} branch misassigned by one quantum. This indicates that only one assignment of the high J lines gives an acceptable fit.

Finally, we carried out a weighted nonlinear least-squares fit including the 1085 lines in the $C^2\Pi$–$X^2\Sigma^+$ (0, 0) band and the 6 microwave transitions in the $X^2\Sigma^+$ v = 0 rotational spectrum measured by Törring and Döbl (*14*). The microwave transitions were given a weight of 10^4 relative to the optical transitions to account for the greater accuracy of the microwave frequencies measured. The 14 parameters determined from this fit are given in Table III along with their two standard deviation errors. The overall standard deviation of this fit is 0.00240 cm^{-1}.

5. DISCUSSION

The molecular constants given in Table II, determined only from the rotational analysis of the $C^2\Pi$–$X^2\Sigma^+$ (0, 0) band, are similar in magnitude to those of Johnson *et al.* (5), except for some higher-order centrifugal distortion constants, which needed to be included to describe the transitions at the higher J'' values.

A comparison of Tables II and III shows that some of the molecular parameters determined in the two fits are quite different. However, both fits are good, with similar

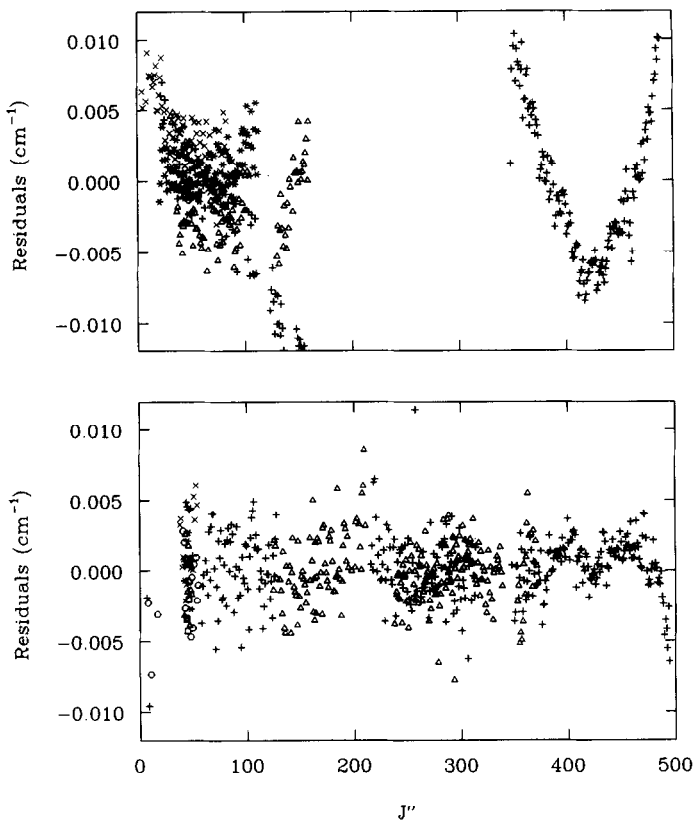

FIG. 6. Residuals of the least-squares fit in which the high J'' section of the P_{12} branch has been misassigned by one unit in J'' to illustrate the systematic trends observed when the assignment is wrong. The upper panel shows the residuals from the $C^2\Pi_{1/2}$–$X^2\Sigma^+$ subband (P_1 (○), P_{12} (+), Q_1 (*), Q_{12} (×), R_1 (△), and R_{12} (□)) and the lower panel shows those from the $C^2\Pi_{3/2}$–$X^2\Sigma^+$ subband (P_{21} (○), P_2 (+), Q_{21} (*), Q_2 (×), R_{21} (△), and R_2 (□)).

standard deviations and no obvious trends in the residuals of the $C^2\Pi$–$X^2\Sigma^+$ (0, 0) rotational branches.

The D'' value determined in the overall fit to the optical and microwave data is much closer to the value predicted by the Kratzer relation $D'' = 4B''^3/\omega_e''^2$ (*15*). For ω_e'' equal to 152.14 cm^{-1} (*14*) this comes to 3.32×10^{-9} cm^{-1}, which we would expect to be a good estimate of D''.

The value of q_0 in both fits seems to be somewhat high, especially in the one including only the optical data. A rough calculation of this constant, based on the unique perturber approximation, would suggest a value of about -4×10^{-7} cm^{-1}, assuming the $D^2\Sigma^+$ state is the perturber (*10, 12*). However, the unique perturber approximation is not expected to be accurate for the $C^2\Pi$ state, because there are at least four $^2\Sigma^+$ states (X, B, D, and E) which are close enough to interact with the $C^2\Pi$ state. We tried a fit in which q_0 was constrained to -4×10^{-7} cm^{-1} while allowing the other 13 parameters to vary. The standard deviation of this fit is 0.00242 cm^{-1} and all the residuals are within the experimental errors. We conclude that with our incomplete data set and the correlations between the parameters used in the fits, we can only determine this constant within an order of magnitude. However, it must be included

TABLE III

Molecular Constants (in cm^{-1}) for the BaI $C^2\Pi$–$X^2\Sigma^+$ (0, 0) Band Determined from a Least-Squares Fit Including the Microwave Data of Törring and Döbl (*14*)

ν_0	1.81784399(155) x 10^4 [a]
A'	7.818559(311) x 10^2
A_D'	-2.39(12) x 10^{-5}
B'	2.671027(98) x 10^{-2}
D'	3.1426(26) x 10^{-9}
H'	3.875(381) x 10^{-16}
q'	-9.4(11) x 10^{-6}
q_D'	1.459(36) x 10^{-10}
p'	7.0357(83) x 10^{-3}
p_D'	-5.567(322) x 10^{-9}
o'	2.5743 x 10^1 calculated
o_D'	-2.037 x 10^{-5} calculated
B"	2.677272(1) x 10^{-2}
D"	3.3331(16) x 10^{-9}
H"	3.647(374) x 10^{-16}
γ"	2.5233(4) x 10^{-3}

[a] Two standard deviation uncertainties derived from the fit are given in parentheses in units of the last significant figure.

to account for the J'' dependence of the frequencies at high J'' values. In the previous analysis of the BaI $C^2\Pi$–$X^2\Sigma^+$ (8, 8) band, a similar problem was noted in the determination of q_0 (*10*).

Table I gives calculated wavenumbers and corresponding J'' values of the six bandheads, determined using each of the two sets of molecular constants, presented in Tables II and III. It is interesting to compare the calculated and experimental bandhead positions, especially in the branches for which there is no information on individual rotational lines with high J'' values. These bandheads are formed mainly because of the difference in the centrifugal distortion constants D' and D''.

The vibrational constant, ω_e'', for the BaI $X^2\Sigma^+$ is 152 cm^{-1}. The rotational energy of a BaI molecule with J'' equal to 494.5 is about 6300 cm^{-1}. Hence, the rotational motion is no longer a small perturbation on the vibrational motion. Calculations show that there are approximately 6 vibrational periods to 1 rotational at $N'' = 494$ as contrasted to close to 2000 vibrational periods for $N'' = 1$. However, we found that the phenomenological Hamiltonians, which are based on perturbation expansions, are able to describe the line positions within their experimental uncertainties.

Another feature of this fit is quite remarkable. We are able to assign unambiguously the rotational quantum numbers of members in a branch when a large number of intermediate members are missing. In our case, for the P_{12} branch, we had 183 lines missing between J'' equal to 156.5 and 338.5, but the assignment was unique. Any other assignment results in a substantial degradation of the quality of the nonlinear

least-squares fit. However, for the P_2 branch, two assignments were possible when 298 lines with J'' values between 50.5 and 347.5 were missing and only 10 lines with J'' values less than 50.5 were available. Additional line positions were necessary to achieve a unique assignment.

APPENDIX

TABLE A1

Rotational and Branch Assignments, Experimental Wavenumbers, and Residuals from the Least-Squares Fit for All New Data

Branch	J"	Experimental Wavenumber (cm-1)	Residual (cm-1)	Branch	J"	Experimental Wavenumber (cm-1)	Residual (cm-1)
P12	339.5	17782.9756	0.0085	P12	397.5	17778.8119	0.0027
	340.5	17782.8920	0.0051		398.5	17778.7494	0.0018
	341.5	17782.8099	0.0028		399.5	17778.6861	-0.0004
	342.5	17782.7296	0.0021		400.5	17778.6265	0.0007
	343.5	17782.6491	0.0010		401.5	17778.5667	0.0012
	344.5	17782.5727	0.0037		402.5	17778.5071	0.0015
	345.5	17782.4956	0.0055		403.5	17778.4473	0.0012
	346.5	17782.4213	0.0097		404.5	17778.3860	-0.0010
	347.5	17782.3239	-0.0093		405.5	17778.3275	-0.0008
	348.5	17782.2520	-0.0032		406.5	17778.2698	-0.0002
	349.5	17782.1816	0.0042		407.5	17778.2126	0.0004
	350.5	17782.0995	-0.0004		408.5	17778.1557	0.0010
	351.5	17782.0238	0.0011		409.5	17778.0980	0.0003
	352.5	17781.9439	-0.0018		410.5	17778.0385	-0.0027
	353.5	17781.8690	0.0000		411.5	17777.9835	-0.0015
	354.5	17781.7925	-0.0001		412.5	17777.9283	-0.0010
	355.5	17781.7160	-0.0005		413.5	17777.8735	-0.0005
	356.5	17781.6391	-0.0016		414.5	17777.8193	0.0001
	357.5	17781.5652	0.0001		415.5	17777.7638	-0.0010
	358.5	17781.4920	0.0021		416.5	17777.7084	-0.0025
	359.5	17781.4124	-0.0025		417.5	17777.6557	-0.0017
	360.5	17781.3393	-0.0010		418.5	17777.6038	-0.0005
	361.5	17781.2652	-0.0007		419.5	17777.5518	0.0001
	362.5	17781.1936	0.0017		420.5	17777.4999	0.0003
	363.5	17781.1208	0.0027		421.5	17777.4487	0.0008
	364.5	17781.0446	-0.0001		422.5	17777.3971	0.0004
	365.5	17780.9707	-0.0008		423.5	17777.3468	0.0009
	366.5	17780.8992	0.0005		424.5	17777.2968	0.0012
	367.5	17780.8268	0.0006		425.5	17777.2473	0.0015
	368.5	17780.7558	0.0018		426.5	17777.1976	0.0011
	369.5	17780.6833	0.0012		427.5	17777.1460	-0.0016
	370.5	17780.6100	-0.0005		428.5	17777.0984	-0.0008
	371.5	17780.5400	0.0007		429.5	17777.0510	-0.0003
	372.5	17780.4692	0.0008		430.5	17777.0043	0.0004
	373.5	17780.3984	0.0006		431.5	17776.9573	0.0004
	374.5	17780.3257	-0.0019		432.5	17776.9116	0.0011
	375.5	17780.2561	-0.0015		433.5	17776.8647	0.0001
	376.5	17780.1875	-0.0006		434.5	17776.8185	-0.0006
	377.5	17780.1192	0.0004		435.5	17776.7742	0.0000
	378.5	17780.0503	0.0004		436.5	17776.7301	0.0004
	379.5	17779.9801	-0.0013		437.5	17776.6875	0.0017
	380.5	17779.9128	-0.0004		438.5	17776.6442	0.0018
	381.5	17779.8459	0.0006		439.5	17776.6024	0.0030
	382.5	17779.7790	0.0012		440.5	17776.5593	0.0023
	383.5	17779.7092	-0.0014		441.5	17776.5166	0.0015
	384.5	17779.6438	0.0000		442.5	17776.4764	0.0026
	385.5	17779.5791	0.0017		443.5	17776.4353	0.0024
	386.5	17779.5133	0.0020		444.5	17776.3950	0.0024
	387.5	17779.4469	0.0013		445.5	17776.3553	0.0024
	388.5	17779.3782	-0.0021		446.5	17776.3153	0.0017
	389.5	17779.3145	-0.0008		447.5	17776.2769	0.0020
	390.5	17779.2514	0.0007		448.5	17776.2381	0.0014
	391.5	17779.1874	0.0009		449.5	17776.2002	0.0011
	392.5	17779.1236	0.0010		450.5	17776.1650	0.0030
	393.5	17779.0593	0.0001		451.5	17776.1263	0.0008
	394.5	17778.9961	0.0000		452.5	17776.0929	0.0034
	395.5	17778.9352	0.0018		453.5	17776.0553	0.0012
	396.5	17778.8731	0.0020		454.5	17776.0226	0.0034

TABLE A1—*Continued*

Branch	J"	Experimental Wavenumber (cm-1)	Residual (cm-1)	Branch	J"	Experimental Wavenumber (cm-1)	Residual (cm-1)
P12	455.5	17775.9890	0.0041	P2	84.5	18562.0982	0.0013
	456.5	17775.9537	0.0025		85.5	18562.0080	0.0023
	457.5	17775.9176	-0.0004		86.5	18561.9164	0.0020
	458.5	17775.8857	0.0003		87.5	18561.8197	-0.0033
	459.5	17775.8506	-0.0028		88.5	18561.7300	-0.0014
	460.5	17775.8199	-0.0020		89.5	18561.6394	-0.0004
	461.5	17775.7921	0.0010		90.5	18561.5509	0.0029
	462.5	17775.7616	0.0008		91.5	18561.4530	-0.0031
	463.5	17775.7335	0.0024		92.5	18561.3631	-0.0009
	464.5	17775.7032	0.0012		93.5	18561.2696	-0.0023
	465.5	17775.6758	0.0023		94.5	18561.1733	-0.0063
	466.5	17775.6468	0.0012		95.5	18561.0878	0.0006
	467.5	17775.6183	0.0001		96.5	18560.9931	-0.0016
	468.5	17775.5918	0.0003		97.5	18560.9003	-0.0018
	469.5	17775.5672	0.0018		98.5	18560.8101	0.0007
	470.5	17775.5391	-0.0008		99.5	18560.7178	0.0013
	471.5	17775.5160	0.0009		100.5	18560.6216	-0.0020
	472.5	17775.4904	-0.0004		101.5	18560.5258	-0.0047
	473.5	17775.4684	0.0013		102.5	18560.4375	0.0002
	474.5	17775.4455	0.0014		103.5	18560.3455	0.0015
	475.5	17775.4217	0.0000		104.5	18560.2538	0.0032
	476.5	17775.4011	0.0011		105.5	18560.1609	0.0038
	477.5	17775.3797	0.0009		106.5	18560.0674	0.0039
	478.5	17775.3586	0.0003		107.5	18559.9705	0.0007
	479.5	17775.3375	-0.0010		108.5	18559.8770	0.0011
	480.5	17775.3192	0.0000		109.5	18559.7822	0.0002
	481.5	17775.3010	0.0003		110.5	18559.6886	0.0007
	482.5	17775.2837	0.0009		111.5	18559.5910	-0.0028
	483.5	17775.2675	0.0020		112.5	18559.4980	-0.0015
	484.5	17775.2498	0.0009		113.5	18559.4038	-0.0014
	485.5	17775.2342	0.0013		114.5	18559.3057	-0.0050
	486.5	17775.2185	0.0009		115.5	18559.2121	-0.0041
P2	57.5	18564.5066	-0.0036		116.5	18559.1192	-0.0023
	58.5	18564.4212	-0.0013		117.5	18559.0260	-0.0007
	59.5	18564.3345	-0.0002		118.5	18558.9304	-0.0015
	61.5	18564.1599	0.0011		119.5	18558.8352	-0.0017
	62.5	18564.0708	0.0002		120.5	18558.7429	0.0010
	63.5	18563.9804	-0.0019		121.5	18558.6431	-0.0036
	64.5	18563.8960	0.0022		122.5	18558.5498	-0.0017
	65.5	18563.8049	-0.0003		123.5	18558.4511	-0.0050
	66.5	18563.7192	0.0027		124.5	18558.3604	-0.0003
	67.5	18563.6313	0.0037		125.5	18558.2634	-0.0018
	68.5	18563.5422	0.0036		126.5	18558.1701	0.0006
	69.5	18563.4498	0.0003		127.5	18558.0763	0.0025
	70.5	18563.3541	-0.0061		215.5	18549.4200	-0.0015
	71.5	18563.2697	-0.0011		216.5	18549.3226	0.0004
	72.5	18563.1777	-0.0036		217.5	18549.2218	-0.0011
	73.5	18563.0936	0.0020		218.5	18549.1285	0.0049
	74.5	18563.0026	0.0007		219.5	18549.0293	0.0049
	75.5	18562.9146	0.0027		220.5	18548.9279	0.0028
	76.5	18562.8190	-0.0029		221.5	18548.8243	-0.0016
	77.5	18562.7295	-0.0022		222.5	18548.7268	0.0001
	78.5	18562.6411	-0.0003		223.5	18548.6283	0.0007
	79.5	18562.5528	0.0018		224.5	18548.5261	-0.0024
	80.5	18562.4571	-0.0033		225.5	18548.4272	-0.0022
	81.5	18562.3716	0.0019		226.5	18548.3294	-0.0009
	82.5	18562.2813	0.0024		227.5	18548.2315	0.0002
	83.5	18562.1870	-0.0010		228.5	18548.1275	-0.0048

TABLE A1—*Continued*

Branch	J"	Experimental Wavenumber (cm-1)	Residual (cm-1)	Branch	J"	Experimental Wavenumber (cm-1)	Residual (cm-1)
P2	229.5	18548.0312	-0.0022	P2	289.5	18542.2291	-0.0001
	230.5	18547.9361	0.0016		290.5	18542.1360	0.0002
	231.5	18547.8344	-0.0012		291.5	18542.0460	0.0034
	232.5	18547.7384	0.0016		292.5	18541.9469	-0.0026
	233.5	18547.6386	0.0006		293.5	18541.8545	-0.0021
	234.5	18547.5371	-0.0022		294.5	18541.7648	0.0010
	235.5	18547.4389	-0.0017		295.5	18541.6687	-0.0025
	236.5	18547.3426	0.0007		296.5	18541.5797	0.0010
	237.5	18547.2443	0.0010		297.5	18541.4856	-0.0008
	238.5	18547.1405	-0.0043		298.5	18541.3972	0.0029
	239.5	18547.0431	-0.0032		299.5	18541.3001	-0.0022
	240.5	18546.9471	-0.0008		300.5	18541.2061	-0.0044
	241.5	18546.8467	-0.0028		301.5	18541.1180	-0.0009
	242.5	18546.7511	-0.0001		302.5	18541.0263	-0.0012
	243.5	18546.6530	0.0001		303.5	18540.9342	-0.0020
	244.5	18546.5558	0.0010		304.5	18540.8472	0.0021
	245.5	18546.4545	-0.0021		305.5	18540.7558	0.0017
	246.5	18546.3577	-0.0009		306.5	18540.6577	-0.0057
	247.5	18546.2617	0.0011		307.5	18540.5733	0.0005
	248.5	18546.1594	-0.0032		308.5	18540.4836	0.0011
	249.5	18546.0624	-0.0024		309.5	18540.3902	-0.0021
	250.5	18545.9687	0.0017		310.5	18540.3041	0.0018
	251.5	18545.8663	-0.0030		311.5	18540.2121	-0.0004
	252.5	18545.7682	-0.0035		312.5	18540.1217	-0.0011
	253.5	18545.6705	-0.0036		313.5	18540.0352	0.0018
	254.5	18545.5764	-0.0002		347.5	18537.1268	0.0011
	256.5	18545.3796	-0.0023		349.5	18536.9608	-0.0029
	257.5	18545.2958	0.0111		350.5	18536.8807	-0.0024
	258.5	18545.1853	-0.0023		351.5	18536.8039	0.0011
	259.5	18545.0890	-0.0015		352.5	18536.7238	0.0010
	260.5	18544.9932	-0.0003		353.5	18536.6412	-0.0019
	261.5	18544.8966	-0.0001		354.5	18536.5639	0.0002
	262.5	18544.7976	-0.0023		355.5	18536.4874	0.0029
	263.5	18544.7016	-0.0016		356.5	18536.4078	0.0021
	264.5	18544.6071	0.0005		357.5	18536.3240	-0.0032
	265.5	18544.5082	-0.0019		358.5	18536.2484	-0.0005
	266.5	18544.4123	-0.0015		359.5	18536.1721	0.0011
	267.5	18544.3167	-0.0008		360.5	18536.0915	-0.0019
	268.5	18544.2204	-0.0009		361.5	18536.0158	-0.0003
	269.5	18544.1213	-0.0039		362.5	18535.9373	-0.0018
	270.5	18544.0279	-0.0014		363.5	18535.8623	-0.0001
	271.5	18543.9365	0.0031		364.5	18535.7881	0.0021
	272.5	18543.8361	-0.0016		365.5	18535.7118	0.0018
	273.5	18543.7402	-0.0019		366.5	18535.6325	-0.0017
	274.5	18543.6476	0.0010		367.5	18535.5592	0.0004
	275.5	18543.5507	-0.0005		368.5	18535.4838	0.0001
	276.5	18543.4540	-0.0019		369.5	18535.4091	0.0001
	277.5	18543.3615	0.0007		370.5	18535.3332	-0.0014
	278.5	18543.2642	-0.0015		371.5	18535.2599	-0.0006
	279.5	18543.1721	0.0013		372.5	18535.1860	-0.0007
	281.5	18542.9816	0.0002		373.5	18535.1127	-0.0006
	282.5	18542.8889	0.0020		374.5	18535.0413	0.0010
	283.5	18542.7942	0.0017		375.5	18534.9634	-0.0041
	284.5	18542.7001	0.0018		376.5	18534.8921	-0.0031
	285.5	18542.6007	-0.0035		377.5	18534.8207	-0.0025
	286.5	18542.5133	0.0031		378.5	18534.7503	-0.0012
	287.5	18542.4172	0.0008		379.5	18534.6787	-0.0015
	288.5	18542.3222	-0.0005		380.5	18534.6089	-0.0003

TABLE A1—*Continued*

Branch	J"	Experimental Wavenumber (cm-1)	Residual (cm-1)	Branch	J"	Experimental Wavenumber (cm-1)	Residual (cm-1)
P2	381.5	18534.5396	0.0010	P2	439.5	18531.1571	-0.0017
	382.5	18534.4700	0.0016		440.5	18531.1139	-0.0007
	383.5	18534.3994	0.0008		441.5	18531.0701	-0.0008
	384.5	18534.3289	-0.0002		442.5	18531.0261	-0.0017
	385.5	18534.2597	-0.0002		443.5	18530.9836	-0.0016
	386.5	18534.1918	0.0006		444.5	18530.9416	-0.0015
	387.5	18534.1232	0.0004		445.5	18530.9002	-0.0014
	388.5	18534.0555	0.0006		446.5	18530.8599	-0.0007
	389.5	18533.9870	-0.0003		447.5	18530.8189	-0.0013
	390.5	18533.9204	0.0004		448.5	18530.7801	-0.0003
	391.5	18533.8531	-0.0001		449.5	18530.7401	-0.0010
	392.5	18533.7872	0.0004		450.5	18530.7007	-0.0017
	393.5	18533.7206	-0.0001		451.5	18530.6623	-0.0020
	394.5	18533.6569	0.0018		452.5	18530.6257	-0.0010
	395.5	18533.5904	0.0006		453.5	18530.5893	-0.0004
	396.5	18533.5251	0.0001		454.5	18530.5529	-0.0004
	397.5	18533.4600	-0.0006		455.5	18530.5171	-0.0004
	398.5	18533.3963	-0.0002		456.5	18530.4811	-0.0011
	399.5	18533.3352	0.0023		457.5	18530.4468	-0.0008
	400.5	18533.2701	0.0004		458.5	18530.4141	0.0006
	401.5	18533.2069	0.0000		459.5	18530.3788	-0.0012
	402.5	18533.1455	0.0009		460.5	18530.3462	-0.0010
	403.5	18533.0837	0.0011		461.5	18530.3138	-0.0011
	404.5	18533.0225	0.0014		462.5	18530.2828	-0.0005
	405.5	18532.9614	0.0014		463.5	18530.2530	0.0008
	406.5	18532.9004	0.0010		464.5	18530.2213	-0.0005
	407.5	18532.8367	-0.0024		465.5	18530.1914	-0.0006
	408.5	18532.7780	-0.0013		466.5	18530.1617	-0.0011
	409.5	18532.7191	-0.0009		467.5	18530.1327	-0.0015
	410.5	18532.6605	-0.0006		468.5	18530.1049	-0.0013
	411.5	18532.6026	0.0000		469.5	18530.0794	0.0005
	412.5	18532.5440	-0.0006		470.5	18530.0540	0.0018
	413.5	18532.4844	-0.0027		471.5	18530.0281	0.0019
	414.5	18532.4281	-0.0018		472.5	18530.0014	0.0006
	415.5	18532.3718	-0.0015		473.5	18529.9745	-0.0015
	416.5	18532.3164	-0.0007		474.5	18529.9495	-0.0024
	417.5	18532.2606	-0.0008		475.5	18529.9262	-0.0022
	418.5	18532.2047	-0.0014		476.5	18529.9037	-0.0019
	419.5	18532.1472	-0.0041		477.5	18529.8823	-0.0011
	420.5	18532.0940	-0.0030		478.5	18529.8619	0.0000
	421.5	18532.0402	-0.0030		479.5	18529.8421	0.0010
	422.5	18531.9876	-0.0022		480.5	18529.8206	-0.0003
	423.5	18531.9349	-0.0020		481.5	18529.8010	-0.0004
	424.5	18531.8828	-0.0017		482.5	18529.7827	0.0001
	425.5	18531.8298	-0.0028		483.5	18529.7639	-0.0005
	426.5	18531.7782	-0.0030		484.5	18529.7469	-0.0001
	427.5	18531.7280	-0.0023		485.5	18529.7296	-0.0006
	428.5	18531.6782	-0.0017		486.5	18529.7142	0.0001
	429.5	18531.6279	-0.0020		487.5	18529.6977	-0.0010
	430.5	18531.5790	-0.0015		488.5	18529.6821	-0.0019
	431.5	18531.5295	-0.0021		489.5	18529.6669	-0.0031
	432.5	18531.4831	-0.0001		490.5	18529.6545	-0.0022
	433.5	18531.4356	0.0003		491.5	18529.6418	-0.0023
	434.5	18531.3878	-0.0001		492.5	18529.6289	-0.0034
	435.5	18531.3376	-0.0034		493.5	18529.6203	-0.0008
	436.5	18531.2929	-0.0018		494.5	18529.6064	-0.0043
	437.5	18531.2468	-0.0021	R21	124.5	18578.0135	-0.0007
	438.5	18531.2024	-0.0012		125.5	18578.0775	0.0028

TABLE A1—*Continued*

Branch	J"	Experimental Wavenumber (cm-1)	Residual (cm-1)	Branch	J"	Experimental Wavenumber (cm-1)	Residual (cm-1)
R21	126.5	18578.1370	0.0019	R21	190.5	18581.7900	0.0031
	127.5	18578.1950	-0.0003		191.5	18581.8437	0.0024
	130.5	18578.3748	-0.0007		192.5	18581.8956	0.0000
	131.5	18578.4338	-0.0015		193.5	18581.9518	0.0020
	132.5	18578.4922	-0.0027		194.5	18582.0040	0.0000
	133.5	18578.5555	0.0010		197.5	18582.1664	0.0001
	134.5	18578.6101	-0.0039		200.5	18582.3276	-0.0004
	135.5	18578.6691	-0.0042		201.5	18582.3849	0.0031
	136.5	18578.7332	0.0006		202.5	18582.4391	0.0035
	138.5	18578.8505	-0.0002		204.5	18582.5460	0.0030
	139.5	18578.9103	0.0007		205.5	18582.5982	0.0016
	140.5	18578.9640	-0.0044		206.5	18582.6500	-0.0002
	141.5	18579.0274	0.0003		207.5	18582.7087	0.0050
	142.5	18579.0878	0.0022		208.5	18582.7631	0.0059
	143.5	18579.1426	-0.0015		209.5	18582.8188	0.0081
	144.5	18579.2012	-0.0013		210.5	18582.8671	0.0030
	145.5	18579.2586	-0.0021		237.5	18584.2917	-0.0044
	146.5	18579.3148	-0.0041		239.5	18584.4005	-0.0013
	147.5	18579.3795	0.0026		240.5	18584.4539	-0.0007
	148.5	18579.4331	-0.0017		241.5	18584.5066	-0.0008
	149.5	18579.4900	-0.0027		242.5	18584.5578	-0.0025
	150.5	18579.5499	-0.0005		243.5	18584.6115	-0.0016
	151.5	18579.6077	-0.0003		244.5	18584.6617	-0.0043
	152.5	18579.6649	-0.0007		245.5	18584.7189	0.0000
	153.5	18579.7217	-0.0013		246.5	18584.7714	-0.0003
	154.5	18579.7779	-0.0025		247.5	18584.8242	-0.0004
	155.5	18579.8360	-0.0016		248.5	18584.8783	0.0008
	158.5	18580.0095	0.0008		249.5	18584.9278	-0.0026
	160.5	18580.1229	0.0005		250.5	18584.9794	-0.0039
	161.5	18580.1800	0.0010		251.5	18585.0360	-0.0003
	162.5	18580.2339	-0.0017		252.5	18585.0906	0.0014
	163.5	18580.2915	-0.0006		253.5	18585.1430	0.0008
	164.5	18580.3481	-0.0004		254.5	18585.1932	-0.0020
	165.5	18580.4073	0.0025		255.5	18585.2467	-0.0016
	166.5	18580.4633	0.0022		256.5	18585.3009	-0.0004
	167.5	18580.5156	-0.0016		257.5	18585.3522	-0.0022
	168.5	18580.5728	-0.0005		258.5	18585.4090	0.0015
	169.5	18580.6262	-0.0030		259.5	18585.4582	-0.0024
	170.5	18580.6879	0.0028		260.5	18585.5147	0.0009
	171.5	18580.7440	0.0031		261.5	18585.5669	-0.0001
	172.5	18580.7970	0.0003		262.5	18585.6214	0.0012
	173.5	18580.8524	0.0001		263.5	18585.6712	-0.0023
	174.5	18580.9066	-0.0013		264.5	18585.7249	-0.0019
	175.5	18580.9623	-0.0011		265.5	18585.7791	-0.0010
	176.5	18581.0205	0.0017		266.5	18585.8357	0.0022
	177.5	18581.0763	0.0022		267.5	18585.8874	0.0005
	178.5	18581.1323	0.0030		268.5	18585.9396	-0.0008
	179.5	18581.1848	0.0003		269.5	18585.9896	-0.0043
	180.5	18581.2376	-0.0020		270.5	18586.0446	-0.0028
	181.5	18581.2932	-0.0015		271.5	18586.0977	-0.0033
	182.5	18581.3489	-0.0007		272.5	18586.1544	-0.0003
	183.5	18581.4040	-0.0005		273.5	18586.2077	-0.0007
	184.5	18581.4652	0.0058		274.5	18586.2616	-0.0006
	185.5	18581.5141	0.0000		275.5	18586.3143	-0.0017
	186.5	18581.5678	-0.0010		276.5	18586.3679	-0.0020
	187.5	18581.6203	-0.0031		277.5	18586.4236	-0.0002
	188.5	18581.6767	-0.0013		278.5	18586.4713	-0.0065
	189.5	18581.7340	0.0015		279.5	18586.5287	-0.0031

TABLE A1—*Continued*

Branch	J"	Experimental Wavenumber (cm-1)	Residual (cm-1)	Branch	J"	Experimental Wavenumber (cm-1)	Residual (cm-1)
R21	280.5	18586.5844	-0.0015	R21	319.5	18588.7640	-0.0011
	281.5	18586.6391	-0.0010		320.5	18588.8234	0.0002
	282.5	18586.6957	0.0013		321.5	18588.8811	-0.0004
	283.5	18586.7521	0.0034		322.5	18588.9365	-0.0034
	284.5	18586.8026	-0.0005		323.5	18588.9949	-0.0036
	285.5	18586.8571	-0.0004		324.5	18589.0557	-0.0015
	286.5	18586.9115	-0.0006		325.5	18589.1171	0.0011
	287.5	18586.9696	0.0029		326.5	18589.1728	-0.0023
	288.5	18587.0226	0.0012		327.5	18589.2338	-0.0004
	289.5	18587.0761	0.0000		328.5	18589.2907	-0.0028
	290.5	18587.1300	-0.0010		329.5	18589.3494	-0.0036
	291.5	18587.1850	-0.0009		330.5	18589.4120	-0.0006
	292.5	18587.2423	0.0014		331.5	18589.4719	-0.0005
	293.5	18587.2930	-0.0030		332.5	18589.5318	-0.0006
	294.5	18587.3512	0.0000		333.5	18589.5926	0.0001
	295.5	18587.4083	0.0018		334.5	18589.6533	0.0005
	296.5	18587.4610	-0.0009		335.5	18589.7133	0.0001
	297.5	18587.5181	0.0008		336.5	18589.7750	0.0012
	298.5	18587.5751	0.0022		337.5	18589.8338	-0.0008
	299.5	18587.6290	0.0004		338.5	18589.8936	-0.0020
	300.5	18587.6840	-0.0003		352.5	18590.7658	-0.0029
	301.5	18587.7427	0.0025		353.5	18590.8313	-0.0013
	302.5	18587.7958	-0.0003		354.5	18590.8905	-0.0061
	303.5	18587.8542	0.0020		355.5	18590.9561	-0.0048
	304.5	18587.9094	0.0010		356.5	18591.0202	-0.0052
	305.5	18587.9649	0.0002		357.5	18591.0864	-0.0037
	306.5	18588.0217	0.0006		358.5	18591.1550	0.0000
	307.5	18588.0785	0.0009		359.5	18591.2183	-0.0019
	308.5	18588.1358	0.0016		360.5	18591.2863	0.0008
	309.5	18588.1915	0.0006		361.5	18591.3536	0.0025
	310.5	18588.2478	0.0000		362.5	18591.4222	0.0052
	311.5	18588.3082	0.0035		363.5	18591.4851	0.0021
	312.5	18588.3612	-0.0006		365.5	18591.6178	0.0020
	313.5	18588.4177	-0.0013		366.5	18591.6805	-0.0021
	314.5	18588.4745	-0.0019		367.5	18591.7522	0.0026
	315.5	18588.5338	-0.0001		368.5	18591.8170	0.0002
	316.5	18588.5932	0.0017		369.5	18591.8864	0.0021
	317.5	18588.6468	-0.0024		370.5	18591.9525	0.0005

ACKNOWLEDGMENTS

P.H.V. thanks the IBM Corporation for support through a postdoctoral fellowship. C.A.L. thanks the SERC for a NATO postdoctoral fellowship. This work was supported by the U.S. National Science Foundation under Grant NSF CHE 89-21198.

RECEIVED: March 1, 1991

REFERENCES

1. O. H. WALTERS AND S. BARRATT, *Proc. R. Soc. London Ser. A.* **118,** 120–137 (1928).
2. M. M. PATEL AND N. R. SHAH, *Indian J. Pure Appl. Phys.* **8,** 681–682 (1970).
3. M. A. JOHNSON, C. R. WEBSTER, AND R. N. ZARE, *J. Chem. Phys.* **75,** 5575–5577 (1981).
4. M. A. JOHNSON AND R. N. ZARE, *J. Chem. Phys.* **82,** 4449–4459 (1985).
5. M. A. JOHNSON, C. NODA, J. S. MCKILLOP, AND R. N. ZARE, *Can. J. Phys.* **62,** 1467–1477 (1984).
6. C. NODA, J. S. MCKILLOP, M. A. JOHNSON, J. R. WALDECK, AND R. N. ZARE, *J. Chem. Phys.* **85,** 856–864 (1986); P. H. VACCARO, D. ZHAO, A. A. TSEKOURAS, C. A. LEACH, AND R. N. ZARE, in preparation.
7. P. H. VACCARO, D. ZHAO, A. A. TSEKOURAS, C. A. LEACH, AND R. N. ZARE, *J. Chem. Phys.* **93,** 8544–8556 (1990).

8. P. J. DAGDIGIAN, H. W. CRUSE, AND R. N. ZARE, *J. Chem. Phys.* **60,** 2330–2339 (1974).
9. S. GERSTENKORN AND P. LUC, "Atlas du spectre d'absorption de la molécule de l'iode," CNRS, Paris, 1978; S. GERSTENKORN AND P. LUC, *Rev. Phys. Appl.* **14,** 791–794 (1979).
10. C. A. LEACH, J. R. WALDECK, C. NODA, J. S. MCKILLOP, AND R. N. ZARE, *J. Mol. Spectrosc.*, **146,** 465–492 (1991).
11. W. E. ERNST, J. KÄNDLER, C. NODA, J. S. MCKILLOP, AND R. N. ZARE, *J. Chem. Phys.* **85,** 3735–3743 (1986).
12. R. N. ZARE, A. L. SCHMELTEKOPF, W. J. HARROP, AND D. L. ALBRITTON, *J. Mol. Spectrosc.* **46,** 37–66 (1973).
13. D. L. ALBRITTON, A. L. SCHMELTEKOPF, AND R. N. ZARE, *in* "Molecular Spectroscopy: Modern Research" (K. Narahari Rao, Ed.), Vol. II, pp. 1–67, Academic Press, New York, 1976.
14. T. TÖRRING AND K. DÖBL, *Chem. Phys. Lett.* **115,** 328–332 (1985).
15. G. HERZBERG, "Molecular Spectra and Molecular Structure. I. Spectra of Diatomic Molecules," Van Nostrand–Reinhold, New York, 1950.